Available online at www.sciencedirect.com

ScienceDirect

journal homepage: www.elsevier.com/locate/he

First-principles studies concerning optimization of hydrogen storage in nanoporous reduced graphite oxide

C.B. Robledo, M.I. Rojas*, O. Cámara, E.P.M. Leiva

INFIQC, Departamento de Matemática y Física, Facultad de Ciencias Químicas, Universidad Nacional de Córdoba, Ciudad Universitaria, 5000 Córdoba, Argentina

ARTICLE INFO

Article history:
Received 26 September 2013
Received in revised form
5 December 2013
Accepted 30 December 2013
Available online 28 January 2014

Keywords:
Hydrogen storage
Reduced graphite oxide
Nanoporous material
Density functional theory

ABSTRACT

By means of Density Functional Theory (DFT) calculations we investigated the optimal pore size for reduced graphite oxide (GOH) to favor hydrogen storage and to prevent oxygen interference. The interlayer distance of GOH is found to increase with oxygen content, given by the number of hydroxyl groups. Four types of GOHs were considered, with O/C ratio within a 0.09–0.38 range. In the case of the highest O/C ratio considered, 0.38, a spontaneous redox-reaction between hydroxyl groups delivering a water molecule and an epoxy group was found. Thus, GOHs with high O/C ratio are not recommended for hydrogen storage. In these materials the absorption energy values of hydrogen is in the range of −0.2 and −0.5 eV/molecule, that is within the values expected to allow an efficient storage. The best GOH for hydrogen storage was found to be that with a 0.09 O/C ratio since it has the largest void space and adequate absorption energy, −0.52 eV/molecule. On the other hand, oxygen absorption energy is lower in absolute value than that of hydrogen, which favors absorption of the latter, thus creating adequate conditions for its storage without oxygen interference.

1. Introduction

Hydrogen is the optimal energy carrier to be employed as vehicular fuel in a new energy economy based on renewable resources. Its heating value is three times higher than that of petroleum and it is a clean fuel since its energy conversion does not produce greenhouse gas effect emissions (GEI) [1,2]. Although their lightness, high specific surface area and low cost make carbonaceous compounds good candidates for hydrogen storage, their storage capacity needs further improvement in order to suit the requirements for vehicular applications. The storage system must be able to safely store the gas at room temperature and at a maximum of 350 bar[1] quickly and must allow numerous cycles of charge/discharge. Thus, the challenge is to develop a carbonaceous material that allows us to store on board four kilograms of hydrogen. Such a material should have both a reasonable volume and weight, allowing an autonomy of over 500 km for a standard fuel cell vehicle [3].

Depending upon the hybridization state of carbon, these materials can bind hydrogen via various mechanisms,

* *Corresponding author*. Tel./fax: +54 (0)351 5353853.
E-mail addresses: mrojas@fcq.unc.edu.ar, marianarojas65@gmail.com (M.I. Rojas).

[1] Pressure used in the storage system of the Honda FCX, fuel cell powered automobile. http://world.honda.com/FuelCell/FCX/tank/.

0360-3199/$ – see front matter
http://dx.doi.org/10.1016/j.ijhydene.2013.12.206

including physisorption, Kubas and chemical bonding. It has been established that the energy per hydrogen molecule must be in the order of 0.1 eV–0.5 eV to establish a reversible absorption/desorption process [4,5]. It has been proposed that hybrid carbon materials decorated with metals may have even higher storage capacities [6,7] than pure carbon materials. Graphite intercalation compounds with alkaline metals also improve the hydrogen storage compared to pristine graphite but it does not fulfill the requirements for mobile applications [8,9]. Nevertheless, there is a significant difference between the theoretical predictions and the experimental measurements, since it has not been possible to reproduce experimentally the storage capacities predicted theoretically. Recently, it has been found through calculations that oxygen traces in the gas phase could strongly interfere with hydrogen storage. This is so because oxygen may either oxidize [10] or block the metallic decorations [11,12].

Although neither pure carbon materials nor hybrid ones suits the requirements for on board applications,[2] mainly concerning gravimetric density, there are promising results related to them [9,11,13]. The problem of oxygen interference could be solved by designing nanoporous materials precluding oxygen access by means of pore-size optimization [14].

Graphite oxide (GO) (stack of several layers of graphene oxide) can be obtained from oxidative-acid treatment of graphite. The most effective experimental synthesis of GO is via the Hummers method [15]. The main reactants used in this method are potassium permanganate, sodium nitrate and sulfuric acid. During the oxidation process, functional groups such as hydroxyl (–OH) and epoxy (–O–) are incorporated into the graphite structure. These groups are responsible for the expansion between graphene planes and for the generation of the split porous structure [16,17]. In experiments, pore dimension in graphite changes from 3.36 to 7.31–7.91 Å depending on the oxidation time [18]. It is possible to control pore size through the oxidation time. On the other hand, Jimenez et al. [14] suggested that hydrogen absorption is improved by functionalization, due to the acid character of the groups, which polarizes the hydrogen molecules. Motivated by these encouraging results, materials derived from graphite oxide were considered in this work as a candidate for hydrogen storage.

In this work we study the properties of reduced graphite oxides (GOH) and their nanoporous structure by means of density functional calculations. The GOH we simulated consisted of pure hydroxyl groups (–OH) defining different oxygen coverage degrees. Hydrogen and oxygen absorption energies are studied in the optimized and expanded geometries (with pores of between 0.6, 0.7 and 0.8 nm). The present work presents essentially two novel results: On one side, we find that the hydrogen binding energy in these systems is between −0.52 and −0.65 eV, that is, very close to the energy window suggested in Refs. [4,5] for optimal hydrogen storage. On the other side, we find that oxygen is not a meaningful interferent in these systems, something that precludes hydrogen adsorption on other systems.

[2] The 2017 DOE target for a promising Hydrogen Storage Material (HSM) is that it should be able to contain a gravimetric density of about 5.5 wt% hydrogen, volumetric capacity of 0.040 kg H_2 L^{-1} and should be able to reversible absorb/desorb H_2 in the temperature range of −40 to 60 °C and moderate pressures (min. 5 bar max. 12 bar). http://www1.eere.energy.gov/hydrogenandfuelcells/storage/pdfs/targets_onboard_hydro_storage.pdf.

2. Calculation

2.1. Computational details

All DFT calculations were performed using the Quantum Espresso package [19] with van der Waals interactions. The Kohn-Sham orbitals and charge density were expanded in plane-waves basis sets up to a kinetic energy cutoff of 35 and 200 Ry for all atoms respectively. Ultra soft pseudopotentials were employed with the Perdew–Wang approximation for exchange and correlation in the PW91 functional [20–22]. The Brillouin zone was sampled with 2 × 2 × 1 irreducible Monkhorst–Pack k-point grid [23]. The convergence threshold for the total energy at each electronic calculations was set to 1×10^{-8} Ry. Geometry optimizations were performed employing the Broyden–Fletcher–Goldfarb–Shanno (BFGS) algorithm (for stress minimization) and total forces acting on each ion were minimized to reach less than 1×10^{-3} Ry/a.u. by movement of the ionic positions.

2.2. The model of GO and GOH

Prior to the investigation of oxidized and reduced structures and with comparative purposes, it was necessary to study graphene sheets and graphite structures. The graphene sheet was simulated with a unit cell with z = 2 nm, so that the plane and its image did not interact; this was done to minimize the C–C distance. In the case of graphite, the structure was composed of stacking sheets of graphene in AB disposition. In order to determine the optimum interlayer distance between graphene sheets, the energy vs. distance was assessed.

The GO and GOH structures were represented by means of a unit cell with two carbon sheets of 32 C atoms each, stacked in an AB arrangement as in the case of graphite. The unit cell was tetragonal $(0.986 \times 0.854 \times z)nm^3$ with periodic boundary conditions in the x,y,z coordinates and the z value was equal to twice the interlayer distance (d). This distance was a function of the O/C ratio.

For GO structures different amounts of epoxy (–O–) and hydroxyl (–OH) groups were randomly arranged to represent amorphous oxides, as it was proposed by Liu et al. [17]. In this work we considered four different amorphous oxides, with a ratio of 2 between functional groups, which are within the

Table 1 – Molecular formula, oxygen/carbon ratio and values of layer adhesion energy of the carbon structures simulated. The average value of the angle between carbon atoms and the hydroxyl group are displayed in the last column.

Substrate	Molecular formula	O/C content	$E_{adhesion}$ [J/m^2]	Angle O–C–C [°]
Graphite	C_{64}	0.00	−0.31	–
GOH1	$C_{64}(OH)_6$	0.09	−0.31	108.2
GOH2	$C_{64}(OH)_{12}$	0.19	−0.51	107.3
GOH3	$C_{64}(OH)_{18}$	0.28	−0.69	108.2
GOH4	$C_{64}(OH)_{24}$	0.38	−1.89	107.9

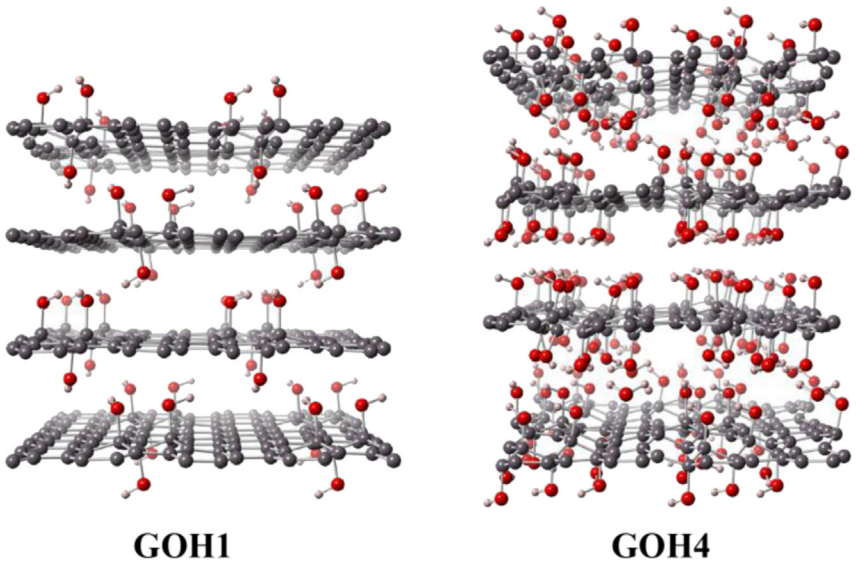

Fig. 1 – Optimized structures of reduced graphite oxide motifs with the lowest (GOH1) and the highest oxygen content (GOH4). Grey: C; red: O; pink: H. (For interpretation of the references to color in this figure legend, the reader is referred to the web version of this article.)

[1.06:3.25] interval of oxides most frequently observed in the experiments.

As the GO structures have epoxy groups, which are highly reactive in the presence of hydrogen, delivering water, we chose reduced graphite oxides to study the properties of inert materials for hydrogen storage. The reduced systems, GOH, were configured by hydrogenating the epoxy sites and thus forming hydroxyl groups. In order to classify them according to the oxygen content, we calculated the O/C ratio in the unit cell. The characteristics of the GOHs studied are compiled in Table 1.

2.3. *Expanded structures*

When investigating the effect of the pore size of GOHs on hydrogen absorption, three different sizes where tried out: 0.6, 0.7 and 0.8 nm. The distance was obtained separating the layers by the desired amount. The expanded structures emulate pillared GOH structures by intercalation of a suitable molecular bridge [24]. Energy minimizations were performed fixing all sp^2 carbon atoms in the z-direction and leaving free the others. Once the minimum energy configuration was obtained, a hydrogen or oxygen molecule was added and the energy was minimized again. In all the cases, the initial absorption site of hydrogen and oxygen molecules, for minimization calculations, was in the center of a six carbons ring (hollow site) as proposed for hydrogen absorption sites in graphite [25,26].

2.4. *Simulation of X-ray diffraction spectra (XRD)*

The graphite interlayer distance can be measured experimentally by X-ray diffraction through the angles at which the diffraction peaks appear, following Bragg's Law:

$$n\lambda = 2d\sin(\theta) \quad (1)$$

where λ is the wavelength of the X-ray diffracted and d is the interlayer distance.

In XRD calculations, the geometry of the GOHX ($X = 1, 2, 3, 4$) crystals was optimized by means of DFT calculations and after that the XRD patterns were simulated using the CrystalDiffract© program.

The physical volume (V_p) of the simulation box was calculated as follows:

$$V_p = d \times S_{GOHX}, \quad (2)$$

where d is the pore width in the z direction and S_{GOHx} is the area of the graphite oxide confined in the box. The total, filled and void space of the simulation box was calculated with the CrystalMaker© program. The void space is thought to be the accessible volume for fluid molecules, such as hydrogen to be stored.

3. Results and discussions

3.1. *Structure*

3.1.1. *Graphene and graphite models*

The minimum energy for the graphene sheet corresponded to $d_{C-C} = 0.142$ nm (0.1415 nm, experimental value). The graphite interlayer distance was 0.320 nm (0.335 nm, experimental value) considering van der Waals interactions in the

Table 2 – Values of 2θ and interlayer distance, d, obtained from simulated X-ray diffraction patterns and characteristics of the unit cell employed.

Substrate	2θ [°]	d [nm]	Total volume [Å^3]	Filled space [%]	Void space [%]
GOH1	19.2	0.465	783.4	17.6	82.4
GOH2	17.5	0.490	825.5	18.3	81.7
GOH3	15.8	0.550	926.6	17.7	82.3
GOH4	15.0	0.570	994.0	17.8	82.2

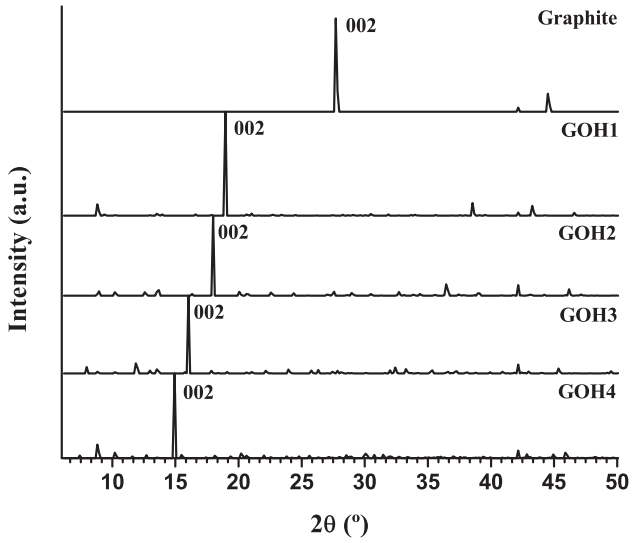

Fig. 2 – Simulated X-ray diffraction patterns for graphite and the different reduced graphite oxides studied.

calculation, which are taken into account in the 4.3.2 version of the Quantum Espresso software.

3.1.2. *GOHs*

Fig. 1 shows the optimized structures for the GOH with the lowest ratio O/C studied (GOH1) and with the highest oxygen content (GOH4). With the increase in the O/C ratio, there are more functional groups, which enlarge both the interlayer distance and the pore size. Upon introducing hydroxyl functionalities into graphite, the planar sp^2 carbon hybridization is locally converted to the tetrahedral sp^3 one, causing local surface undulations. This is reflected in the values of the bond angles between carbon and –OH, whose averages are given in Table 1. They are closer to 109.3° (typical bond angle for sp^3 hybridization), than to the value expected for sp^2 hybridization, i.e. 120°. On the other hand, functionalization produces layer corrugation, which usually reduces the adhesion energy between the carbon layers [27].

It is observed that when the O/C ratio increases so does the volume of the unit cell, due to major interlayer distance. In the case of hydrogen storage, the void space in the cell is important and it should be maximized in order to have more free space for gas absorption. Values for the percent void space are listed in Table 2. Although the void space does not undergo major changes with the O/C ratio, the GOH1 has the largest void space (82.4%), which is convenient for gas storage purposes.

Table 3 – Absorption site of hydrogen and oxygen in the different GOH optimized structures. The subscripts (A) and (B) denote the upper and lower GOH layers respectively.

System	Absorbate	Site
GOH1	H_2	$Hollow_{(A)}$-$Bridge_{(B)}$
	O_2	$Hollow_{(A)}$-$Bridge_{(B)}$
GOH2	H_2	$Top_{(A)}$-$Top_{(B)}$
GOH3	H_2	$Bridge_{(A)}$-$Bridge_{(B)}$
GOH4	H_2	$Bridge_{(A)}$-$Bridge_{(B)}$

The partial structure modification can be inferred from the simulated XRD patterns. Fig. 2 shows the patterns obtained for graphite and the GOHs. We first obtained the diffraction pattern for graphite since it is a well-characterized and known material. As shown in Fig. 2 graphite presents two representative peaks at 26.5° in 2θ, due to the diffraction of the plane 002 and at 44.5° in 2θ due to the diffraction of the plane 041. In the same figure it can be observed that as oxidation is increased in the GOH materials, the peak position for the diffraction peak due to the plane 002 is shifted towards smaller values of 2θ, which gives further indication that the interlayer distance in between planes increases with higher oxygen content. The interlayer distance was calculated using Bragg's Law (eq. (1)). It increases from 0.465 nm in GOH1 to 0.570 nm in GOH4 with higher oxygen content. These values and the corresponding interlayer distances are reported in Table 2, together with characteristics of the unit cell of the material obtained from CrystalMaker®.

In the materials with higher oxygen content, peaks corresponding to diffraction at other planes appear at lower values of 2θ, which do not exist in graphite indicating that the process of functionalization causes distortion of the carbon layers and that a new family of planes is emerging. These findings are similar to those of [28]. The experimental XRD spectrums are more complex than those in Fig. 2 due to the fact that experimental samples have an inhomogeneous mixture of several types of crystals.

In the graphite structure the layers are arranged in AB stacking as shown in Fig. 3A and are bonded to each other by (weak) van der Waals interactions. The adhesion energy

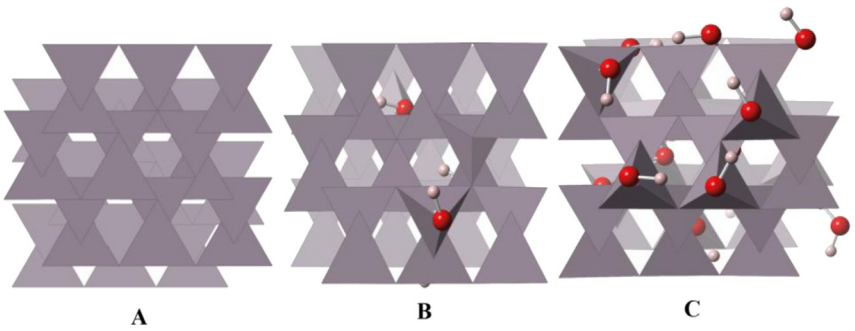

Fig. 3 – View of the structure of a unit cell from the 100 plane of A) Graphite; B) GOH1 and C) GOH4. Grey: C; red: O; pink: H. (For interpretation of the references to color in this figure legend, the reader is referred to the web version of this article.)

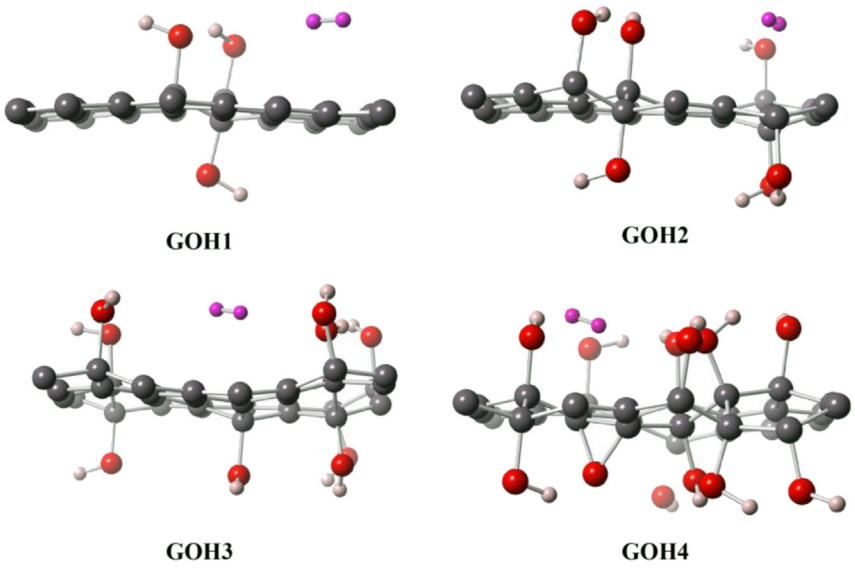

Fig. 4 – Optimized geometry for one hydrogen molecule in the simulated GOHs. Only half a unit cell is shown. The calculations were made for an infinite crystal structure, using periodic boundary conditions. Grey: C; red: O; pink: H; magenta: H_2. (For interpretation of the references to color in this figure legend, the reader is referred to the web version of this article.)

between the graphene planes yields a value of −0.31 J/m^2, which is in agreement with that reported by Bunch [29]. The calculated adhesion energies for the GOH structures are listed in Table 1. It is observed that the adhesion energy between planes increases with the higher oxygen content. We attribute this to hydrogen bond interactions between hydroxyl groups from different layers, which are stronger than van der Waals forces. This allows the layers to expand but not to detach completely from one another. These new interactions are responsible for the progressive modification of the AB stacking form in graphite to AA stacking in the GOH4, as it is shown in Fig. 3. Due to the large amount of −OH groups in GOH4, there is a spontaneous redox reaction between neighboring hydroxyl groups, giving an epoxy group and water according to:

$$2R-OH \rightarrow H_2O + R-O-R' \quad (3)$$

where R–OH represents a hydrogen group attached to a carbon atom and R–O–R′ an epoxy group.

The binding energy of the water molecule in GOH4 was found to be −1.30 eV, characteristic of a strong chemical bond, difficult to remove by straightforward drying.

3.2. *Hydrogen absorption*

The final adsorption sites after energy minimization of the GOHs structure with one molecule of hydrogen located *initially* on hollow with respect to the top carbon layer (A) are listed in Table 3 and the corresponding geometries are shown in Fig. 4. The adsorption sites are assigned with respect to the A and B (the one below A) carbon layers. From the images, it can be observed that in all cases, the H_2 molecule prefers non-functionalized regions, away from the −OH groups, in a zone where the carbon sheets present a local curvature. Particularly, H_2 prefer the concave side of the corrugated carbon plane. Ghosh et al. previously observed this effect and they stated that the presence of a curved carbon surface is one condition for any molecular system to interact effectively with the carbon nanomaterials [30].

Binding energies ($E_b(x)$) for the hydrogen molecules in all the GOHs optimized and expanded structures were calculated as follows:

$$E_b(x) = E_{GOHX-H_2}(x) - E_{GOHX}(x) - E_{H_2}(x), \quad (4)$$

where $E_{GOHX-H_2}(x)$ is the energy of the GOHX with a hydrogen

Table 4 – Absorption energies into reduced graphite oxides as function of the pore size; d_{opt} optimized pore and 0.6; 0.7; 0.8 nm expanded pore.

Substrate	E_{abs} [eV/molecule]				
	Absorbate	E_{abs} (d_{opt})	E_{abs} (0.6 nm)	E_{abs} (0.7 nm)	E_{abs} (0.8 nm)
GOH1	H_2	−0.52	−0.63	−0.61	−0.59
	O_2	−0.26	−0.45	−0.37	−0.31
GOH2	H_2	−0.57	−0.59	−0.65	−0.61
GOH3	H_2	−0.64	−0.57	−0.61	−0.61
GOH4	H_2	−0.22	−0.13	−0.57	−0.61

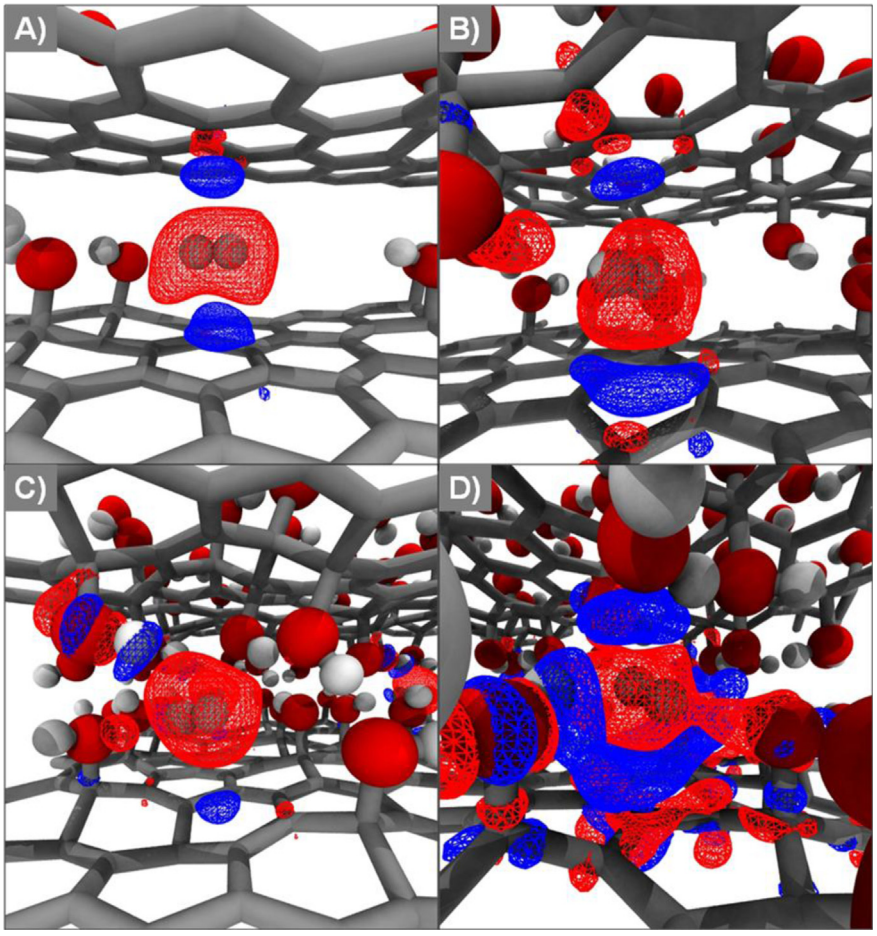

Fig. 5 – Charge density difference plots with an isovalue of 0.0003 e/A^3 due to hydrogen bond formation into A) GOH1; B) GOH2; C) GOH3; D) GOH4. Red and blue iso-surfaces indicate space charge accumulation and depletion, respectively. Grey: C-lattice; red sphere: O; white sphere: H. (For interpretation of the references to color in this figure legend, the reader is referred to the web version of this article.)

molecule into the pore size ($x = 0.6, 0.7, 0.8$, *optimized*), $E_{GOHX}(x)$ corresponds to the GOHX of pore size x and $E_{H_2}(x)$ is the energy of a hydrogen molecule in the same unit cell. Table 4 summarizes the binding energies calculated.

It is observed that the hydrogen absorption energies for the optimized interlayer structures increases in absolute value following the GOH1 < GOH2 < GOH3 sequence. GOH4 shows a drop in the strength of binding energy, absorbing hydrogen with a binding energy of only −0.22 eV, which is low but still within the range suggested for hydrogen storage. The drop in the binding energy of hydrogen could be related to the water present in GOH4. As water formation is not desired, GOH4 does not appear as a suitable hydrogen storage material so it was excluded from further analysis. Compared to graphite, the binding energies of hydrogen in GOHs structures presented in this work are much stronger. One of the important reasons behind the weak interacting nature of hydrogen with graphite can be explained from its electronic structure. The hydrogen molecules has a fully occupied molecular orbital at about −10 eV and has a high ionization potential with low electron affinity, which makes the molecule very stable under normal conditions. Hence, the influence of the neutral graphite surface on the hydrogen molecule is insignificant, but the introduction of oxygen functional groups, forming the reduced graphite oxide structures, seems to favor the interaction with hydrogen. A possible explanation is that the given interaction is through a charge-induced dipole between the GOHs sheets and H_2 molecule. To gain a deeper insight into the interaction mechanism between hydrogen molecules and optimized GOH systems, we evaluated the electronic density difference, $\Delta\rho$, of these materials, which is defined as:

$$\Delta\rho = \rho(\mathrm{GOHX}/\mathrm{H_2}) - \rho(\mathrm{GOHX}) - \rho(\mathrm{H_2}), \quad (5)$$

$\Delta\rho$ plots are shown in Fig. 5, where electron accumulation and depletion regions are represented by red and blue surfaces, respectively. In Fig. 5, a concentration of electronic charge can be observed around the hydrogen molecule, which implies that during hydrogen physisorption some charge has been transferred from the GOH structure to the vicinity of the hydrogen molecule. In this way, a local electric field is formed between the GOH structure and the hydrogen molecule. This particular charge redistribution could be responsible for the relatively strong binding of hydrogen molecules found in the GOHs systems.

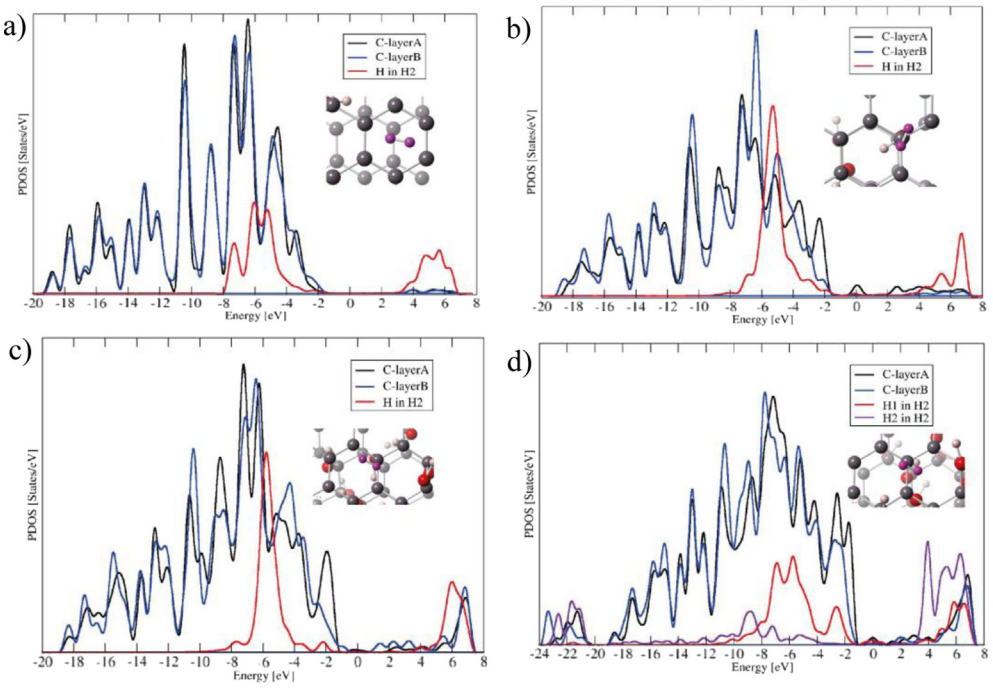

Fig. 6 – PDOS of a) GOH1-H2, b) GOH2-H2, c) GOH3-H2, d) GOH4-H2.

The projected density of states (PDOS) onto H_2 and onto the p_z orbitals of the C atoms of sheets A and B of GOHs adjacent to H_2 are plotted in Fig. 6. It is seen that in all cases the hydrogen molecule interacts with the carbon atoms, allowing the charge redistribution to form the dipole-induced interaction.

In GOH1–GOH3 the strongest absorption energy found was −0.65 eV, which corresponds to GOH2 when the pore size was expanded to 0.7 nm. As previously discussed, the optimum binding energy for hydrogen must be within a −0.2 to −0.5 eV range, since for larger absorption energies too much energy would be necessary to desorb hydrogen molecules which would not be practical for hydrogen storage in safe ambient conditions. Thus, GOH1 without expansion would be the most suitable hydrogen storage system among the ones investigated in this work. We should also note that this material has the highest percentage of void space.

3.3. *Oxygen absorption*

As discussed in the introduction, oxygen has been found to strongly interfere with hydrogen storage in metal-C hybrid systems. We have analyzed potential oxygen interference in the GOH1 system, proposed in this work as the optimum material for the hydrogen storage. Table 3 shows the oxygen absorption energies for GOH1 as a function of porosity, where we considered the same equilibrium interlayer distances for the expanded geometries as for hydrogen absorption. The strength of the absorption bond in the oxygen molecule increases with pore size, being 0.6 nm the optimum, which shows oxygen to be more sensitive than hydrogen to steric effects. The weakest absorption energy is −0.26 eV, which decreases down to −0.45 eV for expanded structures pores. As compared with hydrogen binding energies for GOH1, these values indicate that oxygen does not present a strong interference for hydrogen absorption in these systems.

4. Conclusions

By means of quantum mechanical studies we have investigated the effect of porosity on hydrogen and oxygen absorption into reduced graphite oxide. The latter was evaluated because oxygen is considered a potential interferent for hydrogen storage. Calculations for this material show the size of the pore to increase with the O/C ratio from 0.465 nm to 0.570 nm. Expanded pore structures within a range of [0.6:0.8] nm were also considered.

From the analysis of the present results, it comes out that the reduced graphite oxide with an O/C ratio of 0.09, ($C_{64}(OH)_6$), presents an absorption energy of −0.52 eV/molecule for hydrogen. This quantity slightly increases for expanded structures.

Oxygen absorption energy yields a relatively small value, −0.26 eV/molecule, allowing an optimistic view of hydrogen storage, since oxygen appears as a weak competitor, as opposed to the findings for other carbonaceous related systems.

At a high O/C ratio, water formation was observed, as it is the case of GOH4, which resulted in a reduction of the hydrogen absorption energy. In order to avoid this unwanted effect, low oxygen content is recommended for storage purpose in reduced graphite oxides.

The present results should encourage the experimentalists to make renewed efforts to study hydrogen storage in reduced

graphite oxide, since oxygen interference should be relatively small in these systems.

Acknowledgments

This work was supported by PIP 11420090100066 CONICET, SECyT UNC, PME 2006-1581, Argentina. C. Robledo wishes to thank CONICET for the doctoral fellowship.

REFERENCES

[1] Fayaz H, Saidur R, Razali N, Anuar FS, Saleman AR, Islam MR. An overview of hydrogen as a vehicle fuel. Renew Sust Energ Rev 2012;16(8):5511–28.
[2] Gupta RB. Hydrogen fuel: production, transport and storage; 2009. p. 611.
[3] Ströbel R, Garche ö J, Moseley PT, Jrissen L, Wolf G. Hydrogen storage by carbon materials. J Power Sources 2006;159(2):781–801.
[4] Lochan RC, Head-Gordon M. Computational studies of molecular hydrogen binding affinities: the role of dispersion forces, electrostatics, and orbital interactions. Phys Chem Chem Phys 2006;8(12):1357–70.
[5] Singh AK, Yakobson BI. First principles calculations of H-storage in sorption materials. J Mater Sci 2012;47(21):7356–66.
[6] Durgun E, Dag S, Bagci V, Gülseren O, Yildirim T, Ciraci S. Systematic study of adsorption of single atoms on a carbon nanotube. Phys Rev B 2003;67(20):1–4.
[7] Lopez-Corral I, German E, Juan A, Volpe MA, Brizuela GP. DFT study of hydrogen adsorption on Palladium decorated graphene. J Phys Chem C 2011;115(10):4315–23.
[8] Pinkerton FE, Wicke BG, Olk CH, Tibbetts GG, Meisner GP, Meyer MS, et al. Thermogravimetric measurement of hydrogen absorption in alkali-modified carbon materials. J Phys Chem B 2000 Oct;104(40):9460–7.
[9] Kiyobayashi T, Takeshita HT, Tanaka H, Takeichi N, Züttel A, Schlapbach L, et al. Hydrogen adsorption in carbonaceous materials—: how to determine the storage capacity accurately. J Alloys Compd 2002;330–332(0):666–9.
[10] Rojas M, Leiva E. Density functional theory study of a graphene sheet modified with titanium in contact with different adsorbates. Phys Rev B 2007 Oct;76(15):155415.
[11] Sigal A, Rojas MI, Leiva EPM. Interferents for hydrogen storage on a graphene sheet decorated with nickel: a DFT study. Int J Hydrogen Energy 2011;36(5):3537–46.
[12] Sigal A, Rojas MI, Leiva EPM. Is hydrogen storage possible in metal-doped graphite 2D systems in conditions found on earth? Phys Rev Lett 2011;107(15):158701.
[13] Shiraishi M, Takenobu T, Kataura H, Ata M. Hydrogen adsorption and desorption in carbon nanotube systems and its mechanisms. Appl Phys A 2004;78(7):947–53.
[14] Kim B-J, Park S-J. Optimization of the pore structure of nickel/graphite hybrid materials for hydrogen storage. Int J Hydrogen Energy 2011;36(1):648–53.
[15] Hummers Jr WS, Offeman RE. Preparation of graphitic oxide. J Am Chem Soc 1958;80(6):1339.
[16] Jiménez V, Ramírez-Lucas A, Sánchez P, Valverde JL, Romero A. Improving hydrogen storage in modified carbon materials. Int J Hydrogen Energy 2012;37(5):4144–60.
[17] Liu L, Wang L, Gao J, Zhao J, Gao X, Chen Z. Amorphous structural models for graphene oxides. Carbon 2012;50(4):1690–8.
[18] Wang H, Hu YH. Effect of oxygen content on structures of graphite oxides. Ind Eng Chem Res 2011;50(10):6132–7.
[19] Paolo G, Stefano B, Nicola B, Matteo C, Roberto C, Carlo C, et al. QUANTUM ESPRESSO: a modular and open-source software project for quantum simulations of materials. J Phys Condens Matter 2009;21(39):395502.
[20] Perdew JP, Jackson KA, Pederson MR, Singh DJ, Fiolhais C. Atoms, molecules, solids, and surfaces: applications of the generalized gradient approximation for exchange and correlation. Phys Rev B 1992 Sep 15;46(11):6671–87.
[21] Perdew JP, Wang Y. Accurate and simple analytic representation of the electron-gas correlation energy. Phys Rev B 1992 Jun 15;45(23):13244–9.
[22] Vanderbilt D. Soft self-consistent pseudopotentials in a generalized eigenvalue formalism. Phys Rev B 1990 Apr 15;41(11):7892–5.
[23] Monkhorst HJ, Pack JD. Special points for Brillouin-zone integrations. Phys Rev B 1976 Jun 15;13(12):5188–92.
[24] Kim BH, Hong WG, Moon HR, Lee SM, Kim JM, Kang S, et al. Investigation on the existence of optimum interlayer distance for H2 uptake using pillared-graphene oxide. Int J Hydrogen Energy 2012;37(19):14217–22.
[25] Arellano JS, Molina LM, Rubio a, Alonso J a. Density functional study of adsorption of molecular hydrogen on graphene layers. J Chem Phys 2000;112(18):8114.
[26] Ao ZM, Jiang Q, Zhang RQ, Tan TT, Li S. Al doped graphene: a promising material for hydrogen storage at room temperature. J Appl Phys 2009;105(7):074307.
[27] Huang R. Graphene: show of adhesive strength. Nat Nanotechnol 2011 Sep;6(9):537–8.
[28] Jeong H-K, Lee YP, Lahaye RJWE, Park M-H, An KH, Kim IJ, et al. Evidence of graphitic AB stacking order of graphite oxides. J Am Chem Soc 2008 Jan 30;130(4):1362–6.
[29] Koenig SP, Boddeti NG, Dunn ML, Bunch JS. Ultrastrong adhesion of graphene membranes. Nat Nanotechnol 2011 Sep;6(9):543–6.
[30] Chandrakumar KRS, Srinivasu K, Ghosh SK. Nanoscale curvature-induced hydrogen adsorption in alkali metal doped carbon nanomaterials. J Phys Chem C 2008 Oct 9;112(40):15670–9.